Near- and Deep-Ultraviolet Resonance Raman Spectroscopy of Pyrazine−Al_4 Complex and Al_3−Pyrazine−Al_3 Junction

Mengtao Sun,*,† Shunping Zhang,† Yurui Fang,† Zhilin Yang,†,‡ Deyin Wu,§ Bin Dong,†,∥ and Hongxing Xu†,⊥

Beijing National Laboratory for Condensed Matter Physics, Institute of Physics, Chinese Academy of Sciences, P.O. Box 603-146, Beijing, 100190, People's Republic of China, Department of Physics, State Key Laboratory of Physical Chemistry of Solid Surfaces, and Department of Chemistry, College of Chemistry and Chemical Engineering, Xiamen University, Xiamen 361005, People's Republic of China, School of Science, Dalian Nationalities University, Dalian, 116600, People's Republic of China, and Division of Solid State Physics, Lund University, Lund 22100, Sweden

Received: August 22, 2009; Revised Manuscript Received: September 28, 2009

Near- and deep-ultraviolet (UV) resonance Raman spectroscopy of pyrazine−Al_4 complex and Al_3−pyrazine−Al_3 junction was investigated theoretically with a quantum chemical method. Here, 325 and 244 nm were employed as near- and deep-UV sources in our theoretical study. The intensities of static normal Raman spectra of pyrazine−Al_4 complex and Al_3−pyrazine−Al_3 junction were enhanced on the orders of 10 and 10^3 by a static chemical mechanism, respectively. The calculated absorption spectra reveal strong $^6B_2$ and $^{13}B_{2u}$ electronic transitions near 325 nm for pyrazine−Al_4 complex and 244 nm for Al_3−pyrazine−Al_3 junction, respectively. The analyses of orbital transitions in electronic transitions reveal they are the mixture of (metal to molecule) charge transfer excitation and intracluster excitation. The intensity of near-UV resonance Raman spectroscopy of pyrazine−Al_4 complex and the intensity of deep-UV resonance Raman spectroscopy of Al_3−pyrazine−Al_3 junction are strongly enhanced on the order of 10^5 and 10^4, respectively, compared to the Raman intensity of isolated pyrazine excited at 325 and 244 nm. The calculations of Mie theory and the three-dimensional finite-difference time domain method reveal strong surface plasmon resonance and strong electromagnetic enhancements at 325 and 244 nm for single and dimer nanoparticles at suitable sizes and gap distance, respectively. The strongest SERS enhancement in the system of junction is on the order of 10^8 at the incident lights of 325 and 244 nm. The total enhancements, including the chemical and electromagnetic enhancements, can reach up to 10^{13}. So, Al is a suitable material for near- and deep-UV surface-enhanced resonance Raman scattering.

I. Introduction

Surface-enhanced Raman scattering (SERS) is widely used in chemistry, biology, physics, and material science, since it can enhance the inherently low Raman scattering cross sections of molecules, even at the level of single molecules.[1−5] Extensive investigation of SERS is focused on the Au, Ag, and Cu substrates, which exhibit strong surface plasmon resonance (SPR) in the visible and near-infrared ranges.[6−10] Due to the interband excitation below the wavelength of about 350 and 590 nm for Ag and Au, respectively, the electromagnetic damping results in the weak enhancement of SERS.[11] To extend the applicability of the SERS effect into ultraviolet (UV), other SERS-active metals besides Ag or Au are required that show a plasmonic resonance in the UV.

The investigation of the near- and deep-ultraviolet resonance Raman scattering is rapidly evolving, because of advantages and application in bioscience and material sciences.[12−23] First, the Raman scattering efficiency scales with the fourth power of the frequency. Second, scattering efficiency will be dramatic enhanced when molecules are excited at the molecular electronic absorption bands (resonance Raman scattering) in the UV range. For the preresonance (the wavelength of the laser is close to this resonance) Raman scattering, the relatively high enhancement factors can also be achieved, since the resonance wavelengths is not sharply defined. Third, the UV Raman spectros-

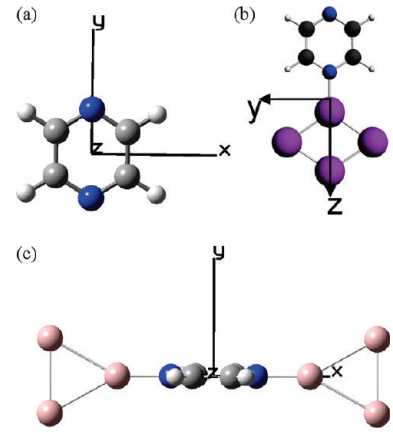

Figure 1. (a) Pyrazine molecule and models of (a) pyrazine−Al_4 complex and (b) Al_3−pyrazine−Al_3 junction. The Cartesian coordinates of them are shown.

* Corresponding author. E-mail: mtsun@aphy.iphy.ac.cn.
† Chinese Academy of Sciences.
‡ Department of Physics, Xiamen University.
§ State Key Laboratory of Physical Chemistry of Solid Surfaces and Department of Chemistry, College of Chemistry and Chemical Engineering, Xiamen University.
∥ Dalian Nationalities University.
⊥ Lund University.

10.1021/jp908107u CCC: $40.75
Published on Web 10/12/2009

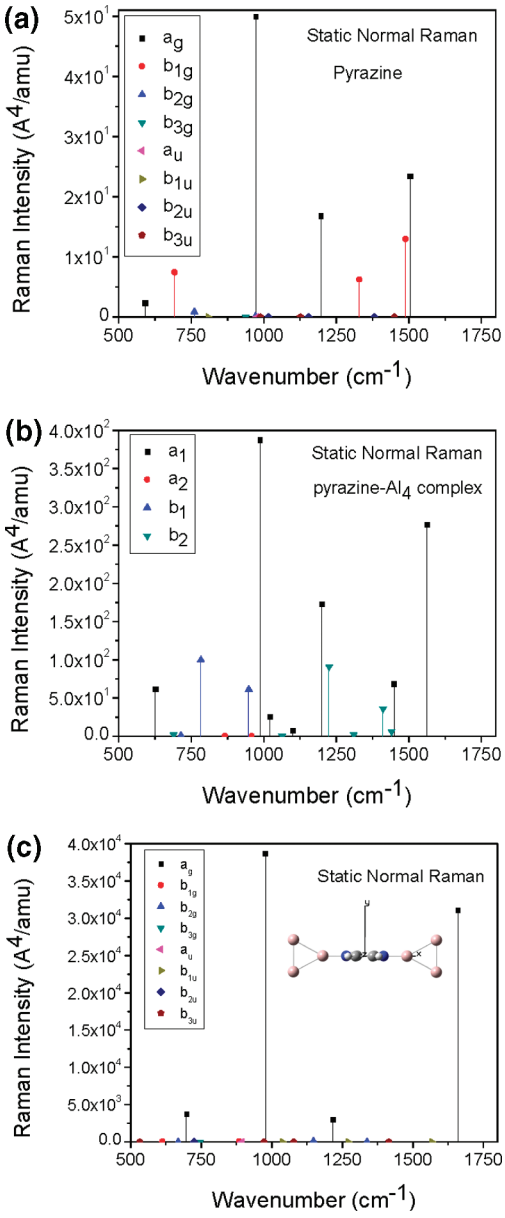

Figure 2. Static normal Raman scattering spectra of (a) pyrazine, (b) pyrazine−Al_4 complex, and (c) Al_3−pyrazine−Al_3 junction.

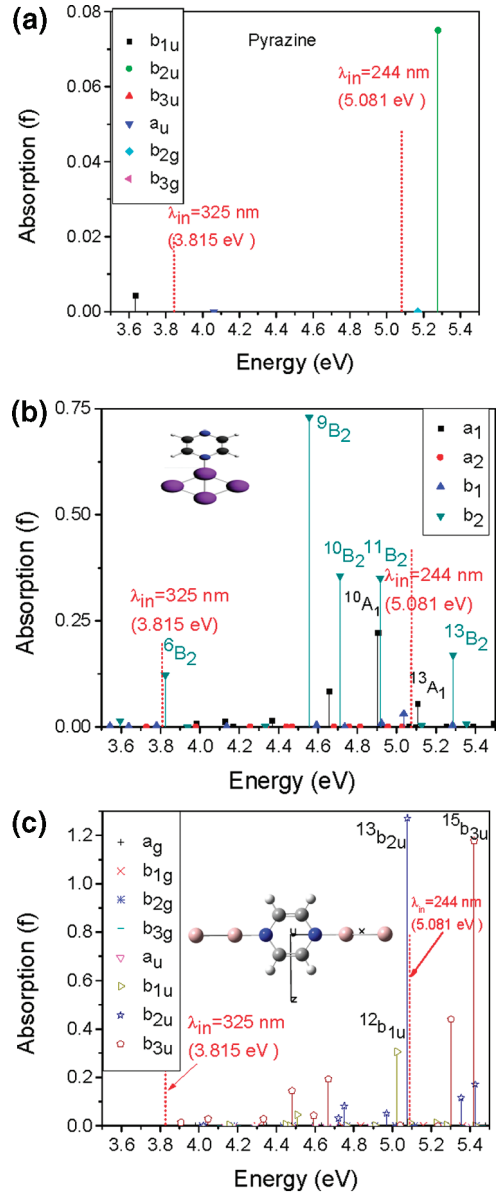

Figure 3. (a) Absorption spectra of (a) pyrazine, (b) pyrazine−Al_4 complex, and (c) Al_3−pyrazine−Al_3 junction in the range of 3.5−5.5 eV.

TABLE 1: Calculated Static Electronic Polarizability Components (in au)

	xx	*yy*	*zz*
pyrazine	73.9	66.7	31.5
pyrazine−Al_4 complex	139.6	329.2	479.8
Al_3−pyrazine−Al_3 junction	1094.6	320.5	282.4

copy is not interfered by fluorescence; since there is no material that fluoresces below the wavelength of 280 nm, then the fluorescence and Raman spectra are completely separated at an excitation wavelength below 260 nm.[12]

In the search for UV−SERS material, aluminum (Al) is one of best candidates, because it has low absorption down to a wavelength of 200 nm due to its free-electron-like character and plasmon resonance in UV range,[11] but such experimental and theoretical investigation is quite limited. Experimentally, Dörfer and co-workers demonstrated the capability of an aluminum surface to be SERS-active for deep-UV excitation wavelengths.[24] Ekinic et al. found that Al nanostructures exhibit strong plasmon resonances in the UV range.[25] Taguchi et al. reported the tip enhancement of resonance Raman scattering using deep-ultraviolet excitation wavelength.[18] The tip enhancement was successfully demonstrated with an aluminum-coated silicon tip that acts as a plasmonic material in deep-UV wavelengths.[18] Shashilov and Lednev studied 2D correlation deep-UV resonance Raman spectroscopy of early events of lysozyme fibrillation.[23] Theoretically, Zeman predicted theoretically that Al ellipsoids enable strong Raman scattering enhancement factors in the UV range.[26]

The pyrazine molecule is an important probe molecule in the SERS field, and the SERS of pyrazine has been extensively investigated experimentally and theoretically,[27−31] which is suitable to study the coupling effect of metals in metal−pyrazine−metal junction systems, due to the bonding interaction between nitrogen atoms and two metal electrodes. Recent experimental and theoretical findings indicate that large SERS enhancements have been observed for molecules interacting with small nanocluster or nanocrystalline semiconductor surface.[32−34] We have studied the chemical mechanism of surface-enhanced resonance Raman scattering (SERRS) via charge transfer in

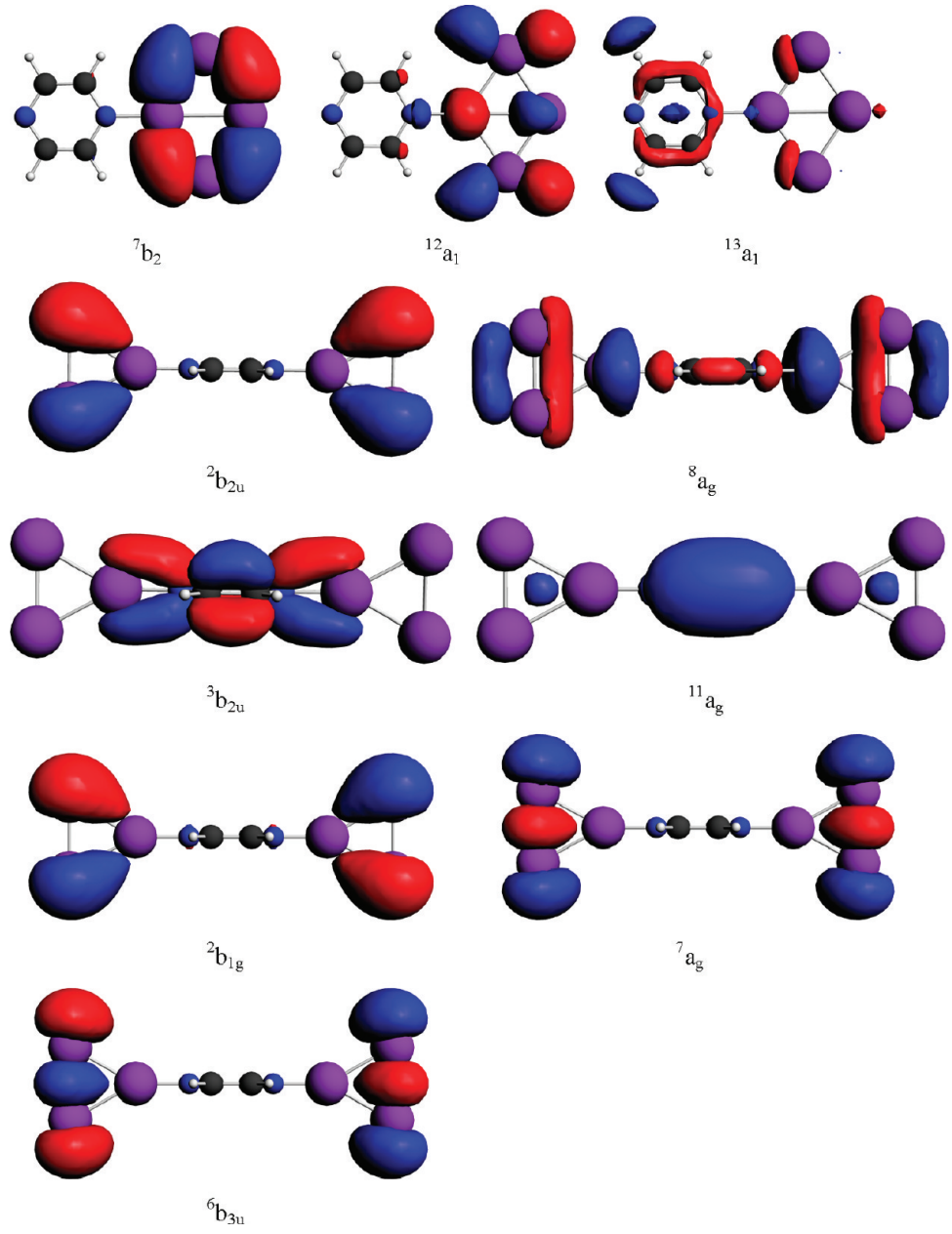

Figure 4. Molecular orbitals of pyrazine−Al_4 complex and Al_3−pyrazine−Al_3 junction in the $^{6}B_2$ and $^{13}B_{2u}$ electronic transitions near 325 and 244 nm, respectively, where the blue and red stand for different phases of wave functions.

TABLE 2: Electronic Transitions of $^{6}B_2$ and $^{13}B_{2u}$ with Large Oscillator Strength for Pyrazine−Al_4 Complex and Al_3−Pyrazine−Al_3 Junction, Respectively

	vibrational modes	eV	components of orbital transitions
pyrazine−Al_4 complex	$^{6}B_2$	3.8245	77.7% ($^{7}b_2 \rightarrow {}^{13}a_1$); 11.1% ($^{7}b_2 \rightarrow {}^{12}a_1$)
Al_3−pyrazine−Al_3 junction	$^{13}B_{2u}$	5.0773	22.7% ($^{2}b_{2u} \rightarrow {}^{8}a_g$); 11.3%($^{3}b_{2u} \rightarrow {}^{11}a_g$); 10.4% ($^{2}b_{2u} \rightarrow {}^{6}b_{3u}$); 10.1% ($^{2}b_{1g} \rightarrow {}^{7}a_g$)

PATP−metal (metal = Au_5 or Ag_5) complex and metal−PATP−metal junction,[35] and tunneling charge transfer in metal−PATP−metal junction at the incident light of 1064 nm was visualized with charge difference density. The resonance enhancement and the charge transfer mechanism play important roles. So, models of pyrazine−Al_n complex and Al_n−pyrazine−Al_n junction ($n \leq 10$) may be suitable to simultaneously simulate the charge-transfer enhancement and resonance Raman spectroscopy of molecules adsorbed on the Al substrate.

In this paper, with quantum chemical methods, we theoretically study the near- and deep-UV resonance Raman spectroscopy of pyrazine−Al_4 complex and Al_3−pyrazine−Al_3 junction. Here, 325 and 244 nm were employed as near- and deep-UV sources in our theoretical study. Strong chemical enhancement via charge transfer at the incident lights of 325 and 244 nm were revealed theoretically. With generalized Mie theory, SPR of Al single particle and particle dimer were tuned to 325 and 244 nm by their size or separation (for dimer), while local electric field enhancement was carried at each resonance by the three-dimensional finite-difference time domain method (3D-FDTD) method.

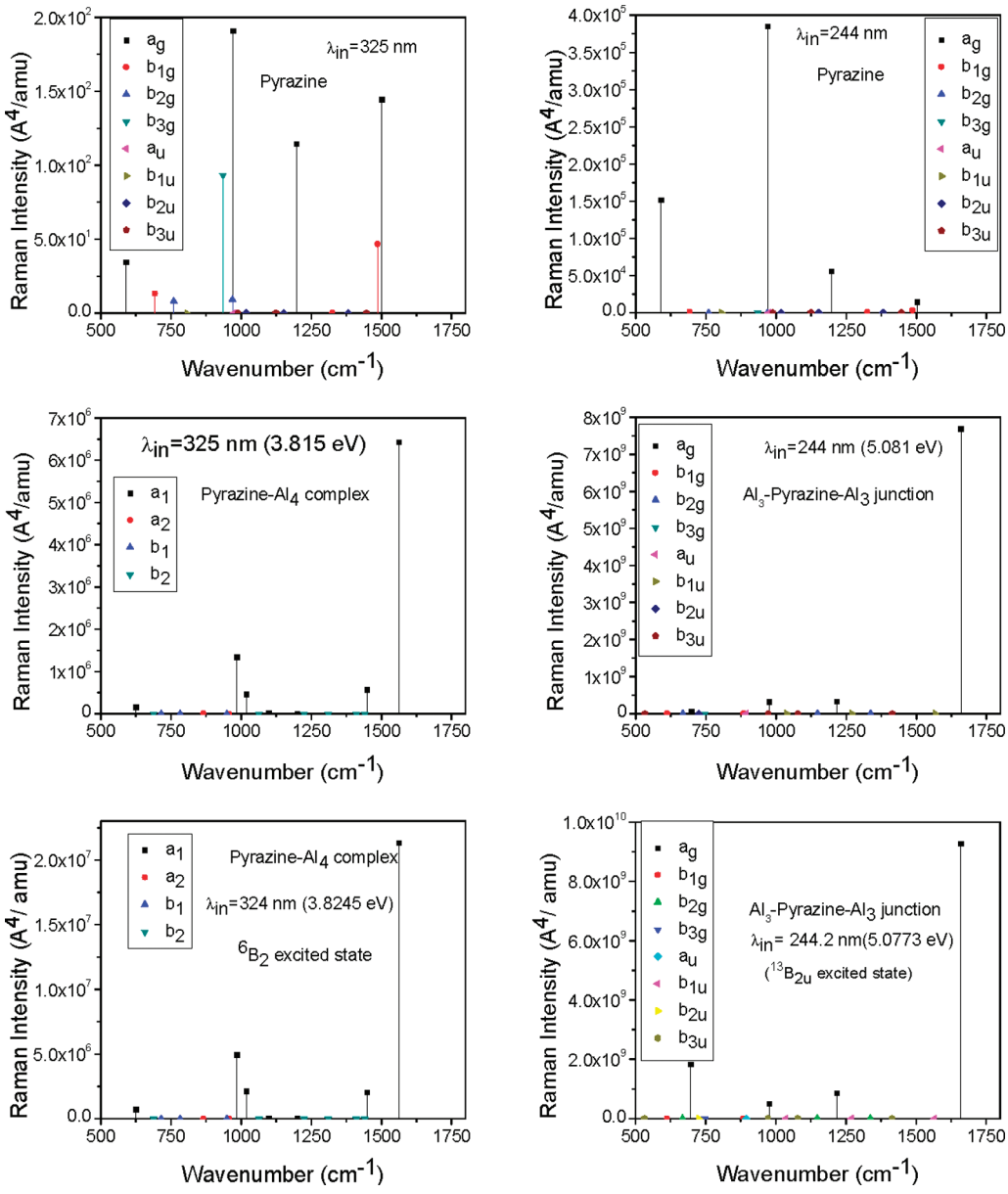

Figure 5. Resonance Raman spectra of pyrazine, pyrazine−Al_4 complex, and Al_3−pyrazine−Al_3 junction at 325 and 244 nm.

II. Methods

All quantum chemical calculations were performed with Amsterdam density functional (ADF) suite.[36] Models of pyrazine−Al_4 and Al_3−pyrazine−Al_3 were used as molecule−Al complex and Al−molecule−Al junction (see Figure 1), where pyrazine, pyrzaine−Al_4 complex, and Al_3−pyrazine−Al_3 junction are D_{2h}, C_{2v}, and D_{2h} symmetry, respectively. The molecular structures of them were calculated at the density functional theory (DFT)[37] level of theory using the gradient-corrected Becke−Perdew (BP86) exchange-correlation functional.[38] A triplet-ζ polarized Slarter-type (TZP) basis set has been used to optimize ground-state geometry. A full electron basis set has been used for N, C, and H, whereas the 2p core has been frozen for Al. The absorption spectra of them were calculated with time-dependent density functional theory (TD-DFT),[39] using the same functional and basis set. In the calculations of electronic transitions, only singlet−singlet excitations were evaluated. The vibrational frequencies and normal nodes are calculated within the harmonic approximation. The BP86 functional often gives harmonic frequencies that are close to experimental values.[40] The static normal Raman and resonant Raman spectra of isolated pyrazine, pyrazine−Al_4 complex, and Al_3−pyrazine−Al_3 junction were calculated at zero frequency and 325 and 244 nm, respectively.

To confirm that aluminum nanoparticle could be a candidate for SERS in near- and deep-UV regains, we perform electromagnetic simulations of both single sphere and sphere dimer, based on generalized Mie theory.[41] SPR can be effortlessly tuned by varying their size and separation; we can shift their resonance to 242 and 316 nm for single sphere and 325 and 248 nm for sphere dimer, according to the applied light sources. The maximum order of multipole in the simulation was set to more than 22 and 25 for singlet and dimer, respectively. The dielectric constants of Al were taken from ref 11.

For quantitative estimate of the electromagnetic enhancement at the near-field region, we used the 3D-FDTD method[42] to calculate the local electric field distribution of Al spheres at the special frequency, namely 244 and 325 nm. In this method, the space containing the simulated model is discretized using elements called the "yee cell". The number of periods of the

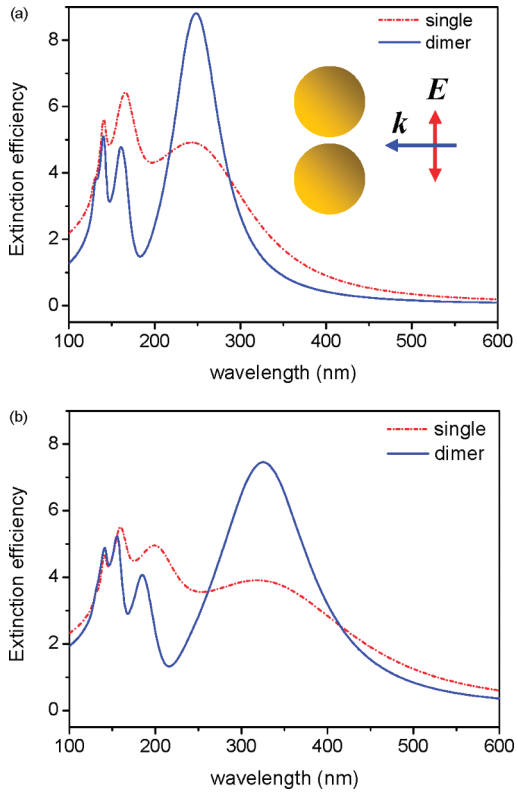

Figure 6. Far-field extinction spectrum of single aluminum nanosphere (dash) and sphere dimer (solid). Dipolar resonance peaks were tuned toward 244 nm (a) and 325 nm (b). The radius of a single sphere is $R_1 = 39$ nm, while those of the dimer are $R_2 = 20$ nm, with gap $G = 1.5$ nm in (a), in contrast to $R_1 = 55$ nm, $R_2 = 30$ nm, $G = 1.2$ nm in part b. The incident plane wave for particle dimer is show in the inset.

incident sinusoidal plane wave was set to 10 to guarantee calculation convergence, which could be judged by checking whether near-zone electric field values had reached a steady state. The amplitude of the sinusoidal plane wave was set to be 1 V/m in the calculation. All FDTD calculations were conducted in the platform of a commercial XFDTD software package (RemCom XFDTD 6.3).

III. Results and Discussion

A. Ground-State Properties. Due to the interaction between pyrazine and Al, the polarizabilities of pyrazine−Al_4 complex and Al_3−pyrazine−Al_3 junction are significantly enhanced (see data in Table 1), which results in strong enhancement of the intensity of the static normal Raman scattering spectroscopy for pyrazine−Al_4 complex and Al_3−pyrazine−Al_3 junction, compared to that of pyrazine (see Figure 2). The enhanced orders are 10 and 10^3 for pyrazine−Al_4 complex and Al_3−pyrazine−Al_3 junction, respectively. So, the coupling effect of the junction is very important for the Raman intensity. Note that the frequency of 1505 cm^{-1} (a_g mode) of pyrazine shifted to 1563 cm^{-1} (a_1 mode) and 1659 cm^{-1} (a_g mode) for pyrazine−Al_4 complex and Al_3−pyrazine−Al_3 junction, respectively.

B. Near- and Deep-UV Electronic Transition Properties. The absorption spectroscopy in Figure 3a demonstrates that there is no electronic resonance excitation at 325 nm, while at 244 nm, there is a near-resonant excitation for isolated pyrazine. From Figure 3b, there is a near-resonant excitation at 325 nm (3.815 eV), which is close to $^6B_2$ electronic transition at 3.8245 eV for pyrazine−Al_4 complex. The energy difference between 325 nm (3.815 eV) and $^6B_{2u}$ electronic transition (3.8245 eV) is only 0.0095 eV, so the Raman spectroscopy of pyrazine−Al_4 complex at the incident light of 325 nm should be resonant Raman spectroscopy.

Close to the $^{13}B_{2u}$ electronic transition at 5.0773 eV, Raman spectroscopy of Al_3−pyrazine−Al_3 junction at the incident light of 244 nm (5.081 eV) is preresonance Raman. Since the energy difference between 244 nm (5.081 eV) and $^{13}B_{2u}$ electronic transition (5.0773 eV) is only 0.0037 eV, we can consider that the Raman spectroscopy of Al_3−pyrazine−Al_3 junction at the incident light of 244 nm is the resonant Raman spectroscopy.

According to the components of orbital transitions in electronic excitations and the density of state on these orbitals (see them in Table 2 and Figure 4), they are the mixture of metal to molecule charge transfer excitation and intracluster excitation, and the dominant contribution is charge-transfer excitation. If the cluster size is large enough, charge-transfer excitation and intracluster excitation are the mechanisms of chemical and electromagnetic enhancement, respectively.

C. Near- and Deep-UV Resonant Raman Spectra. To calculate the Raman enhanced factors, the Raman spectra of isolated pyrazine at 325 and 244 nm were calculated (see Figure 5a). It is found that the Raman intensity at 325 nm is only slightly enhanced by 4 times that of the static normal Raman (see Figure 2a), and the Raman profile of them is quite similar. While the Raman intensity at 244 nm is strongly enhanced, compared to the intensities of the static normal Raman spectroscopy, and the enhanced order is 10^4, the Raman profile of them is significantly different. The reason can be interpreted by the absorption of pyrazine. There is no electronic resonance excitation at 325 nm, while at 244 nm, there is a near resonant excitation (see Figure 5a).

Since the incident light of 325 nm (3.815 eV) is close to the $^6B_2$ electronic transition at 3.8245 eV for pyrazine−Al_4 complex, we calculated the preresonance Raman spectroscopy of pyrazine−Al complex at 325 nm, which can be seen in Figure 5c. By comparing parts a and c for Figure 5, three conclusions can be obtained: (1) the enhanced order of resonance Raman intensity is 10^5, resulting from the resonant enhancement via metal to molecule charge transfer; (2) their profiles are significant different, which is the spectroscopy evidence for a charge-transfer enhanced mechanism; and (3) the 1563 cm^{-1} (a_1 mode) band is the dominantly enhanced one, since it corresponds to the vibrational motion of the nitrogen atoms along the Ag−N bond. We also calculated the resonance Raman spectroscopy at 3.8245 eV ($^6B_2$ electronic transition) for pyrazine−Al_4 complex (see Figure 5e). It is found that the profile of preresonant Raman spectroscopy at 325 nm is very similar to the profile of resonance Raman spectroscopy at 3.8245 eV ($^6B_2$ electronic transition), but the intensity of preresonant Raman spectroscopy is one-third that at $^6B_2$ electronic transition (3.8245 eV).

We also calculated the preresonance Raman spectroscopy of Al_3−pyrazine−Al_3 junction at 244 nm (see Figure 5d), which is significantly different from the preresonance Raman of pyrazine at 244 nm. Because of metal to molecule charge transfer (chemical mechanism), the intensity of resonance Raman spectroscopy of Al_3−pyrazine−Al_3 junction is enhanced at the level of 10^4, compared to that of preresonant Raman spectroscopy of isolated pyrazine at the incident light of 244 nm. Since the energy difference between 244 nm (5.081 eV) and $^{13}B_{2u}$ electronic transition (5.0773 eV) is only 0.0037 eV, not only are the profiles of their Raman spectra very similar but also their Raman intensities are almost the same.

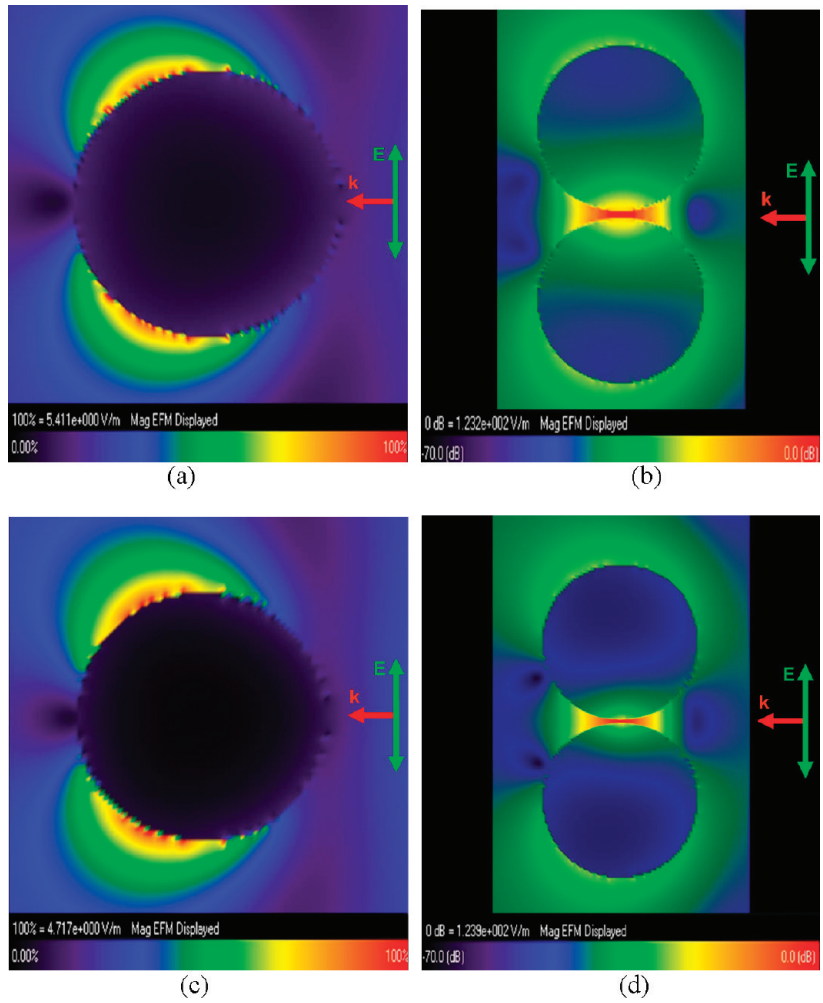

Figure 7. Near electric field distribution of aluminum nanosphere: (a) single sphere and (b) sphere dimer at $\lambda = 244$ nm, with the same geometric parameter as in Figure 6a; (c) single sphere and (d) sphere dimer at $\lambda = 325$ nm, with the parameter given in Figure 6b. The incident plane wave for particle dimer is show in the inset.

D. Near- and Deep-UV Extinction Spectroscopy Near-Field Distribution. Since surface plasmon resonance of metal nanoparticles can be effortlessly tuned by varying their size and separation, we can shift their resonance toward to 244 and 325 nm for single sphere and sphere dimer. Far-field extinction spectrum of single aluminum nanosphere and sphere dimer can be seen in Figure 6, where dipolar resonance peaks were tuned toward 244 nm (Figure 6a) and 325 nm (Figure 6b). When the radius of a single sphere is 39 nm and those of the dimer are 20 nm with a gap of 1.5 nm, the SPR peak can be tuned to near 244 nm. When the radius of a single sphere is 55 nm and the radius of sphere dimer is 30 nm with a gap of 1.2 nm, the SPR peak can be tuned to near 325 nm.

Figure 7a,b demonstrates the near-field distribution at 244 nm for single sphere and sphere dimer with the same size and gap distance as in Figure 6a. The strongest electromagnetic enhancements are $|M|^2 = 2.93 \times 10^1$ ($|M|^2 = |E_{local}/E_0|^2$) and $|M|^2 = 1.52 \times 10^4$ for single sphere and sphere dimer, respectively. The enhancements of SERS are $|M|^4 = 8.58 \times 10^2$ and $|M|^4 = 2.31 \times 10^8$, respectively. Figure 7c,d demonstrates the near-field distribution at 325 nm for single sphere and sphere dimer with the same size and gap distance as in Figure 6b. The strongest electromagnetic enhancements are $|M|^2 = 2.23 \times 10^1$ and $|M|^2 = 1.54 \times 10^4$ for single sphere and sphere dimer, respectively. The enhancements of SERS are $|M|^4 = 4.97 \times 10^2$ and $|M|^4 = 2.37 \times 10^8$, respectively.

IV. Conclusion

Quantum chemical results revealed that intensities of static normal Raman spectra of pyrazine−Al_4 complex and Al_3−pyrazine−Al_3 junction were enhanced on the orders of 10 and 10^3 by a static chemical mechanism, respectively. So, the coupling effect by the junction is very important for the Raman intensity. The intensity of near-UV resonance Raman spectroscopy of pyrazine−Al_4 complex and the intensity of deep-UV resonance Raman spectroscopy of Al_3−pyrazine−Al_3 junction are strongly enhanced by on the order of 10^5 and 10^4, respectively, compared to the Raman intensity of isolated pyrazine excited at 325 and 244 nm. The SPR peak can be tuned to 325 and 244 nm by controlling the size and gap distance of nanospheres, and SERS enhancement can reach on the order of 10^2 ($|M|^4$) for single and 10^8 ($|M|^4$) for dimer nanoparticles at 325 and 244 nm. So, Al is a suitable material for near- and deep-UV surface-enhanced resonance Raman scattering. The total enhancements, including the chemical and electromagnetic enhancements, can reach up to 10^{13}.

Acknowledgment. This work was supported by the National Natural Science Foundation of China (Grant Nos. 90923003, 10874234, 20703064, 20703032, 10625418, and 10804015), the National Basic Research Project of China (Grant Nos. 2009CB930701, 2009CB930703, and 2007CB936804), and the Natural Science Foundation of Fujian Province of China (Grant No. E0710028).

References and Notes

(1) Metiu, H.; Dos, P. *Annu. Rev. Phys. Chem.* **1984**, *35*, 507.
(2) Moskovits, M. *Rev. Mod. Phys.* **1985**, *57*, 783.
(3) Otto, A.; Mrozek, I.; Grabhorn, H.; Akeman, W. *J. Phys.: Condens. Matter* **1992**, *4*, 1143.
(4) Kneipp, K.; Wang, Y.; Kneipp, H.; Perelman, L. T.; Itzkan, I.; Dasari, R.; Feld, M. S. *Phys. Rev. Lett.* **1997**, *78*, 1667.
(5) Xu, H. X.; Bjerneld, E. J.; Kail, M.; Borjesson, L. *Phys. Rev. Lett.* **1999**, *83*, 4357.
(6) Lombardi, J. R.; Birke, R. L.; Lu, T.; Xu, J. *J. Chem. Phys.* **1986**, *84*, 4174.
(7) Fleischmann, M.; Hendra, P. J.; McQuillan, A. J. *Chem. Phys. Lett.* **1974**, *26*, 163.
(8) Jeanmaire, D. J.; Van Duyne, R. P. *J. Elektroanal. Chem.* **1977**, *84*, 1.
(9) Campion, A.; Kambhampati, P. *Chem. Soc. Rev.* **1998**, *27*, 241.
(10) Willets, K. A.; Van Duyne, R. P. *Annu. Rev. Phys. Chem.* **2007**, *58*, 267.
(11) Palik, E. D. (Ed.) *Handbook of Optical Constants of Solids*; Academic: Orlando, FL, 1985.
(12) Asher, S. A. *Anal. Chem.* **1993**, *65*, 59A. *Anal. Chem.* **1993**, *65*, 201A.
(13) Fodor, S. P. A.; Spiro, T. G. *J. Am. Chem. Soc.* **1986**, *108*, 3198.
(14) Lin, X.-F.; Ren, B.; Yang, Z. L.; Liu, G. K.; Tian, Z. Q. *J. Raman Spectrosc.* **2005**, *36*, 606.
(15) Ren, B.; Lin, X. F.; Yang, Z. L.; Liu, G. K.; Aroca, R. F.; Mao, B. W.; Tian, Z. Q. *J. Am. Chem. Soc.* **2003**, *125*, 9598.
(16) Hecht, L.; Clarkson, J.; Smith, B. J. E.; Springett, R. *J. Raman Spectrosc.* **2007**, *37*, 562.
(17) Tian, Z. Q.; Yang, Z. L.; Ren, B.; Wu, D.-Y. SERS from transition metals and excited by ultraviolet light. In *Surface-Enhanced Raman Scattering-Physics and Applications*; Kneip, K., Moskovits, M., Kneip, H., Eds.; Topics Applied Physics; Springer-Verlag: New York, 2006; Vol. 103, 125.
(18) Taguchi, A.; Hayazawa, N.; Furusawa, K.; Ishitobi, H.; Kawata, S. *J. Raman Spectrosc.* **2009**, *40*, 1324.
(19) Konorov, S. O.; Schulze, H.; Addison, C. J.; Haynes, C. A.; Blades, M. W.; Turner, R. F. B. *J. Raman Spectrosc.* **2009**, *40*, 1162.
(20) Shafaat, H. S.; Sanchez, K. M.; Neary, T. J.; Kim, J. E. *J. Raman Spectrosc.* **2009**, *40*, 1060.
(21) Fujiwara, A.; Mizutani, Y. *J. Raman Spectrosc.* **2008**, *39*, 1600.
(22) Huang, C.; Balakrishnan, G.; Spiro, T. G. *J. Raman Spectrosc.* **2006**, *37*, 277.
(23) Shashilov, V.; Lednev, I. K. *J. Am. Chem. Soc.* **2008**, *130*, 309.
(24) Dorfer, T.; Schmitt, M.; Popp, J. *J. Raman Spectrosc.* **2007**, *38*, 1379.
(25) Ekinci, Y.; Solak, H. H.; David, C. *Opt. Lett.* **2007**, *32*, 172.
(26) Zeman, E. J.; Schatz, G. C. *J. Phys. Chem.* **1987**, *91*, 634.
(27) Arenas, J. F.; Woolley, M. S.; Tocon, I. L.; Otero, J. C.; Marcos, J. I. *J. Chem. Phys.* **2000**, *112*, 7669.
(28) Arenas, J. F.; Woolley, M. S.; Otero, J. C.; Marcos, J. I. *J. Phys. Chem.* **1996**, *100*, 3199.
(29) Zhao, L. L.; Jensen, L.; Schatz, G. C. *Nano Lett.* **2006**, *6*, 1229.
(30) Sun, M. T.; Li, Z. P.; Liu, Y. J.; Xu, H. X. *J. Raman Spectrosc.* In press (DOI: 10.1002/jrs.2344).
(31) Tian, Z. Q. *J. Raman Spectrosc.* **2005**, *36*, 466.
(32) Peyser-Capadona, L.; Zheng, J.; Gonzalez, J. L.; Lee, T. H.; Patel, S. A.; Dickson, R. M. *Phys. Rev. Lett.* **2005**, *94*, 058301.
(33) Zheng, J.; Ding, Y.; Tian, B.; Wang, Z. L.; Zhuang, X. *J. Am. Chem. Soc.* **2008**, *130*, 10472.
(34) Yang, L.; Jiang, X.; Ruan, W.; Zhao, B.; Xu, W.; Lombardi, J. R. *J. Phys. Chem. C* **2008**, *112*, 20095.
(35) Sun, M. T.; Xu, H. X. *ChemPhysChem* **2009**, *10*, 392.
(36) te Velde, G.; Bickelhaupt, F. M.; Baerends, E. J.; Guerra, C. F.; van Gisbergen, S. J. A.; Snijders, J. G.; Ziegler, T. *J. Comput. Chem.* **2001**, *21*, 931; ADF, 2008.
(37) Dreizler, R. M.; Gross, E. K. U. *Density Functional Theory, an Approach to the Quantum Many-Body Problem*; Springer-Verlag: Berlin, 1990.
(38) Becke, A. D. *Phys. Rev. A.* **1988**, *38*, 3098. Perdew, J. P. *Phys. Rev. B* **1986**, *33*, 8822.
(39) Gross, E. K. U.; Kohn, W. *Phys. Rev. Lett.* **1985**, *55*, 2850.
(40) Neugebaur, J.; Hess, B. A. *J. Chem. Phys.* **2003**, *118*, 7215.
(41) Xu, H. X. *Phys. Lett. A* **2003**, *312*, 411.
(42) Kunzr, K. S.; Luebber, R. J. *The Finite Difference Time Domain Method for Electromagnetics*; CRC: Cleveland, 1993.

JP908107U